A novel numerical model to predict the morphological behavior of magnetic liquid marbles using coarse grained molecular dynamics concepts

Hasitha-Nayanajith Polwaththe-Gallage, Emilie Sauret, Nam-Trung Nguyen, Suvash C. Saha, and YuanTong Gu

Citation: Physics of Fluids **30**, 017105 (2018);
View online: https://doi.org/10.1063/1.5000289
View Table of Contents: http://aip.scitation.org/toc/phf/30/1
Published by the American Institute of Physics

A novel numerical model to predict the morphological behavior of magnetic liquid marbles using coarse grained molecular dynamics concepts

Hasitha-Nayanajith Polwaththe-Gallage,[1] Emilie Sauret,[1,a)] Nam-Trung Nguyen,[2] Suvash C. Saha,[1] and YuanTong Gu[1]
[1]*School of Chemistry, Physics and Mechanical Engineering, Faculty of Science and Engineering, Queensland University of Technology, 2 George Street, Brisbane, QLD 4001, Australia*
[2]*Queensland Micro- and Nanotechnology Centre, Griffith University, 170 Kessels Road, Nathan, QLD 4111, Australia*

(Received 15 August 2017; accepted 20 December 2017; published online 22 January 2018)

Liquid marbles are liquid droplets coated with superhydrophobic powders whose morphology is governed by the gravitational and surface tension forces. Small liquid marbles take spherical shapes, while larger liquid marbles exhibit puddle shapes due to the dominance of gravitational forces. Liquid marbles coated with hydrophobic magnetic powders respond to an external magnetic field. This unique feature of magnetic liquid marbles is very attractive for digital microfluidics and drug delivery systems. Several experimental studies have reported the behavior of the liquid marbles. However, the complete behavior of liquid marbles under various environmental conditions is yet to be understood. Modeling techniques can be used to predict the properties and the behavior of the liquid marbles effectively and efficiently. A robust liquid marble model will inspire new experiments and provide new insights. This paper presents a novel numerical modeling technique to predict the morphology of magnetic liquid marbles based on coarse grained molecular dynamics concepts. The proposed model is employed to predict the changes in height of a magnetic liquid marble against its width and compared with the experimental data. The model predictions agree well with the experimental findings. Subsequently, the relationship between the morphology of a liquid marble with the properties of the liquid is investigated. Furthermore, the developed model is capable of simulating the reversible process of opening and closing of the magnetic liquid marble under the action of a magnetic force. The scaling analysis shows that the model predictions are consistent with the scaling laws. Finally, the proposed model is used to assess the compressibility of the liquid marbles. The proposed modeling approach has the potential to be a powerful tool to predict the behavior of magnetic liquid marbles serving as bioreactors. *Published by AIP Publishing.* https://doi.org/10.1063/1.5000289

I. INTRODUCTION

Liquid marbles are liquid droplets coated with superhydrophobic powder.[1,2] Liquid droplets are rolled on a superhydrophobic powder bed to form liquid marbles. Once the liquid marble is formed, the solid particle layer at the liquid-air interface separates the liquid from the surrounding environment.[1,3] This layer is not rigid and deforms according to the morphology of the droplet. Therefore, liquid marbles can be characterized using the elastic solid models, which contain liquid inside a soft solid membrane. Various research groups have investigated the properties and behavior of liquid marbles under different conditions. The liquid marbles with a radius less than the capillary length, $k^{-1} = \sqrt{\gamma/\rho g}$, (where γ is the surface tension of the liquid marble, ρ is the density of the liquid, and g is the acceleration of gravity) exhibit a quasi-spherical shape as the gravity becomes negligible compared to the surface tension forces.[1,4] When the volume of the liquid marble increases, the gravity becomes dominant and liquid marbles exhibit puddle-shapes.[5,6] The effective surface tension of water marbles has been calculated with the aid of experimental results,[1,2] and it has been found that the effective surface tension of the water marbles is less than the effective surface tension of water droplets (γ = 0.072 N/m). The reduction of the effective surface tension of the water marbles occurs due to the presence of solid particles at the liquid-air interface.[7]

Liquid marbles pose unusual physical properties and characteristics. It has been found that the liquid marbles remain stable and retain their non-stick properties on both solid and liquid supports.[8] Recent experiments showed that water marbles coated with lycopodium particles submerge in polydimethylsiloxane.[9] The liquid marbles coated by polyvinylidene fluoride float on water, but they are destroyed when the water is contaminated with kerosene or silicon oil,[10,11] while the liquid marbles coated with poly(2-vinylpyridine) exhibit pH-sensitivity.[12] These marbles show long-term stability when they are placed on a surface of liquid water of pH 4.9 or above.[12] On the other hand, they disintegrate when the pH is less than 2.9.[12] This physical behavior of liquid marbles highly depends on the properties of the coated particles.[8] Thanks to those behaviors, it has been reported that liquid marbles have been used in gas sensing[13] and miniaturized chemical

a)Electronic mail: emilie.sauret@qut.edu.au.

processes.[7] Recent studies demonstrated the use of liquid marbles as bioreactors for three-dimensional cell culture,[14] which is currently one of the most promising applications of liquid marbles.

Magnetic liquid marbles are formed by rolling liquid droplets on a superhydrophobic magnetic powder such as Fe_3O_4. These magnetic liquid marbles are highly responsive to external magnetic fields, and they can be opened and closed reversibly[7] with an external magnetic field. These features make the magnetic liquid marble as a potential alternative to conventional discrete microfluidic systems,[15] and these magnetic liquid marbles have high potential to be used in applications related to biomedical and drug delivery.[1] However, the magnetic powder of the magnetic liquid marbles does not serve as a solid phase substrate for molecular tagging since they remain on the surface of the liquid droplet[16] and do not allow for complex bioassays that require liquid exchange. Still, it is believed that the surface-functionalized magnetic particles can be utilized for affinity binding with no effect to the operation of liquid marbles.[16]

Liquid marbles are relatively new microfluidic platforms, and the complete behavior of liquid marbles under various environmental conditions is yet to be studied. However, in order to understand the complete behavior of liquid marbles, cost-intensive and time consuming experiments have to be performed. A robust and accurate modeling approach is a good solution to overcome this problem and will help to predict and analyze the behavior of liquid marbles with ease. Vigorous models always inspire new experiments and provide new insights.

Analytical models have been used to characterize the deformation of floating liquid marbles by Ooi *et al.*[2] Wong *et al.*[17] employed a modeling approach to show that the floating state of the liquid marbles heavily depends on the interfacial tension of the particle coating. However, these models assumed that the interface of the floating liquid marble completely behaves like a liquid droplet. The numerical modeling techniques can be easily and effectively used to predict and explain the behavior of liquid marbles under different external conditions and environments. To the best of our knowledge, there is no numerical model developed to simulate the morphological changes in the liquid marbles. The two main numerical modeling techniques available to simulate the physical phenomena are grid-based techniques (such as Finite Element Method; FEM and Finite Volume Method; FVM) and meshfree particle methods (such as Smoothed Particle Method; SPH, Lattice Boltzmann Method; LBM, Coarse Grained Molecular Dynamics; CGMD, Immersed Boundary Method; IBM, and Discrete Element Method; DEM).[18] The meshfree particle methods are more capable of effectively modeling multiphase phenomena.[19] Therefore, the proposed model will use CGMD concepts and will be the first numerical model developed based on the particle methods to simulate and predict the behavior of magnetic liquid marbles under external magnetic fields. The application of CGMD concepts to model the liquid marbles gives flexibility of adding any physics (such as fluid dynamics, thermodynamics, and electromagnetism) to the model with ease.

This paper begins with the modeling concepts and the formulation of the liquid marble model. For validation purpose, the developed model is used to predict the changes in the height of a magnetic liquid marble against its horizontal diameter and compared with experimental results. It can be seen in Sec. III A that the model predictions are highly comparable both qualitatively and quantitatively with the experimental findings. The morphology of a liquid marble directly depends on the surface tension of the liquid, the density of the liquid, the density of the coating material, and gravity.[10] These parameters are independent from each other, and in this study, the acceleration of gravity is set to 9.8 m/s^2. A comprehensive parametric study is carried out to evaluate the effect of other individual parameters on the morphology of the liquid marbles. Thereby the dominant parameters which govern the morphology of the liquid marbles are identified as the surface tension and the density of the liquid. Then, the model is employed to simulate the reversible process of opening and closing of the magnetic liquid marble under the action of a magnetic force. This feature of the liquid marble demonstrates their potential in digital microfluidics and drug delivery. Finally in Sec. III H, the proposed model is employed to demonstrate the elastic nature of the liquid marbles. The proposed model is the first to demonstrate capabilities to model such unique microfluidic platforms.

II. MODEL DEVELOPMENT

The magnetic liquid marble is assumed to be a soft elastic solid object,[1] which contains liquid inside a soft solid membrane. In order to develop a simple and computationally efficient model, this model adapts the concepts used in red blood cell modeling.[20] We consider a liquid marble coated with a layer of superhydrophobic Fe_3O_4 nanoparticles. Generally, liquid marbles exhibit axis-symmetrical shapes [see Fig. 1(a)]. For instance, the geometry of the liquid marble in Fig. 1(a)

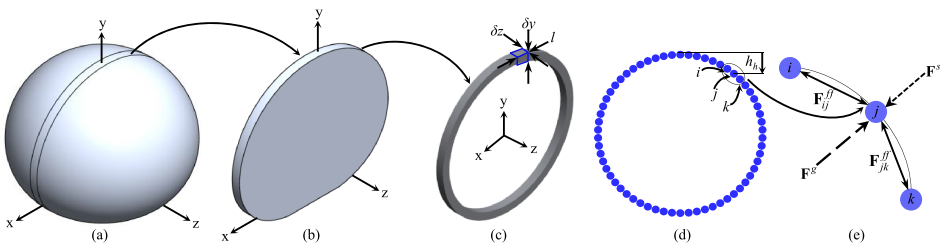

FIG. 1. (a) The axis-symmetrical shape of a typical liquid marble. (b) The cross section of the liquid marble chosen to model. (c) The initial shape of the liquid marble model is assumed to be a sphere and simplified into a thin walled cylinder. (d) Particle representation of the liquid droplet. (e) Forces acting on liquid particles due to the weight of the liquid; F^g, surface tension; F^s, and the particle to particle interaction; F^{ff}.

is symmetric around the y-axis. Due to the axis symmetrical nature of the liquid marbles, a cross section of the liquid marble (from xy-plane) is chosen as the model, Fig. 1(b). By rotating this cross section around the y-axis, the geometrical shape of the whole liquid marble can be obtained. This simplification does not affect the model predictions as long as liquid marbles exhibit axis-symmetrical shapes. More importantly, this simplification reduces the computational cost significantly without affecting the final output. However, in order to precisely predict the complex three-dimensional (3D) asymmetric behaviors of the liquid marbles, 3D modeling techniques have to be used. In this model, the initial shape of the liquid marble is assumed to be a sphere, and the shape of the cross section is simplified into a circle. The liquid marble is modeled by two layers: the inside layer represents the outer surface of the liquid droplet and the outside layer represents the solid nanoparticle layer. Then, the forces acting on the two layers (outer liquid surface layer and Fe_3O_4 nanoparticle layer) of the liquid marble are analyzed and calculated based on the surface tension and the gravitational forces. In addition to the above forces, the particle to particle interactions between two layers and the particle to particle interactions in the Fe_3O_4 nanoparticle layer are also taken into the account.

A. Representation of the outer surface of the liquid droplet

Initially, the inner layer of the model is isolated and the forces acting on the outer surface of the liquid droplet are investigated. In this study, a cross section of the liquid droplet [see Fig. 1(b)] is modeled and it is simplified into a finite thin walled hollow cylinder with a height, δz, and a thickness, δy [see Fig. 1(c)]. Here, δz is a critical parameter, and it should be small enough to represent the whole liquid marble by a finite thin walled hollow cylinder. In this study, the Cartesian coordinate system is used to develop the liquid marble model. The Cartesian coordinate system can be directly transformed into either polar or cylindrical coordinate system, whenever it is required. However, the final model predictions do not depend on the coordinate system since the governing equations of the model are not influenced by the coordinate system. In this CGMD modeling approach, the problem domain is discretized into a set of particles and the forces acting on them are calculated based on their positions in the problem domain. Moreover, the particle-based CGMD model does not use the continuum-based partial differential equations. Therefore, as long as the shape of the liquid marble is axis-symmetrical, the liquid marble can be represented by a finite thin walled hollow cylinder.

The wall of the thin walled hollow cylinder is then discretized into a set of particles [see Fig. 1(d)]. In order to conserve the volume of the liquid droplet, the area enclosed by the particles is conserved and the formula used in red blood cell modeling[20] is used to calculate the forces acting on each particle due to the areal conservation as

$$\mathbf{F}^a = k_a \frac{\partial}{2\partial \mathbf{r}} \left(\frac{A - A_0}{A_0} \right)^2, \tag{1}$$

where A and A_0 are the present and the original areas of the liquid droplet, respectively, while $\boldsymbol{r}$ is the position vector of the particle of interest and k_a is the area constraint coefficient. Equation (1) allows us to model the whole liquid droplet without employing additional liquid particles to model the inside of the liquid droplet. Moreover, it aids to maintain a uniform area throughout whole simulation, and the change in the area can be further minimized by using a larger k_a value. However, the number of particles used to represent the liquid marble should be large enough to precisely calculate the area of the liquid marbles with higher local curvatures. It should be noted that both the liquid marbles and the red blood cells are considered to be soft elastic solid objects.[1] Therefore, the equation established to represent the interaction between the particles in red blood cell modeling can be directly used to develop the liquid marble model. The surface area and the volume of the red blood cells do not change with the external forces, but the surface area of the liquid marble changes with the external forces. Therefore, an additional numerical function has to be implemented to facilitate the changes in the surface area of the liquid marbles. Moreover, the size of the liquid marble is larger compared to the dimensions of the red blood cells. Therefore, the parameters have to be adjusted precisely so that the model can predict the realistic behavior of the liquid marbles.

Due to the area conservation, the distance between consecutive liquid particles increases, when the liquid droplet shows any shape other than a circle. Therefore, in order to maintain uniform distance between consecutive liquid particles, interaction forces ($\mathbf{F}^{ff}$) are introduced,

$$\mathbf{F}^{ff} = k_l \frac{\partial}{2\partial \mathbf{r}} \left(\frac{l - l_0}{l_0} \right)^2, \tag{2}$$

where l is the present length between two consecutive particles and k_l can be defined as the uniform length coefficient, while l_0 is the present mean distance between two consecutive particles and is updated by

$$l_0 = \frac{1}{n} \sum_{i=1}^{n} l, \tag{3}$$

where n is the number of particles used to model the liquid droplet. As can be seen in Fig. 1(e), the interaction force between particles i and j, $\mathbf{F}_{ij}^{ff}$, acts on particles i and j in the opposite direction but equal in magnitude.

The shape of the liquid droplet is governed by the gravitational and surface tension forces. First, the hydrostatic pressure on each particle due to the weight of the liquid droplet itself is calculated by

$$p^g = h_h \rho g, \tag{4}$$

where h_h is the height from the topmost point of the liquid droplet to the particle at which the hydrostatic pressure is required to be calculated. Then, the force acting on that particle due to the weight of the liquid droplet is calculated by

$$\mathbf{F}^g = p^g l_0 \delta z. \tag{5}$$

The surface tension forces help us to keep the spherical shape of the liquid droplet without dispersing. Next, an external pressure is applied on each particle to prevent the motion of the particles in the outward normal direction to the surface of the liquid droplet. This pressure is calculated using the

Young-Laplace equation,

$$p^s = \gamma\left(\frac{1}{r_1} + \frac{1}{r_2}\right), \tag{6}$$

where r_1 and r_2 are the principal radii of curvatures. In this model, for a thin walled hollow cylinder, the Young-Laplace equation can be modified as $p^s = \gamma/r$ (since the radii of curvatures of the thin walled hollow cylinder in yz- and xz-planes are infinity), where r is the radius of curvature of the thin walled hollow cylinder in the xy-plane [see Fig. 1(e)]. Subsequently, the force acting on the particle is calculated by

$$\mathbf{F}^s = p^s l_0 \delta z. \tag{7}$$

However, when the liquid droplets exhibit puddle shapes, l_0 increases due to the area conservation. It leads to increase in the error during the calculation of curvature. In order to minimize the error, the above equation is modified to

$$\mathbf{F}^s = p^s l_0 \delta z\,(l_0/l_i), \tag{8}$$

where l_i is the initial mean distance between two consecutive particles, when the liquid droplet has a circular shape.

B. Representation of the particle coating of the liquid marble

The shapes of the Fe_3O_4 nanoparticles are assumed to be spherical with an average diameter (d) of 10.2 nm as reported in the experimental study.[1] The solid nanoparticle layer of the liquid marble is modeled by another set of particles with finite mass. It should be noted that one particle in the model represents a cluster of Fe_3O_4 nanoparticles with a uniform diameter of 10.2 nm. In order to model the interaction forces ($\mathbf{F}^{sl}$) between solid and fluid particles, the modified Lennard-Jones (LJ) type forces are employed as

$$\mathbf{F}^{sl} = \frac{f_0^{sl}}{r^{sl}}\left[\left(\frac{r_0^{sl}}{r^{sl}}\right)^{13} - \left(\frac{r_0^{sl}}{r^{sl}}\right)^{7}\right], \tag{9}$$

where r^{sl} and r_0^{sl} are the present and the original distances between the solid and the liquid particles, respectively, while f_0^{sl} is the strength of the LJ contact for solid-liquid interaction. These LJ forces are acting pair-wisely in the opposite directions on solid and liquid particles. The application of LJ type forces is more appropriate in order to avoid the penetration of solid particles through the liquid surface. Furthermore, these forces aid to maintain a constant gap between solid and liquid particles. In this model, virtual particle concepts[21] are used to determine r^{sl}. As can be seen in Fig. 2, the LJ interaction force between solid particle c and the liquid droplet is $\mathbf{F}_c^{sl}$. The distance from solid particle, c, to the surface of the liquid droplet is the perpendicular distance (shortest distance) from the solid particle c to the ij line segment, that is, the distance between the virtual particle, vp, and the solid particle, c. The calculated $\mathbf{F}_c^{sl}$ is then directly applied on the solid particle, while it is distributed on liquid particles, i and j, depending on the distance from the virtual particle, vp, to the liquid particles, i and j. In Fig. 2, x_1 and x_2 are the distances from the virtual particle vp to liquid particles i and j, respectively. In order to model the

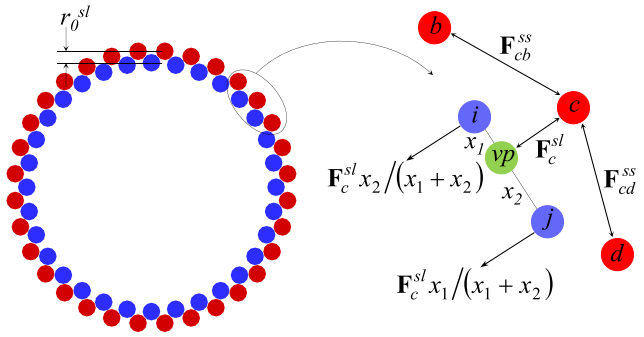

FIG. 2. Interaction forces between solid particles (red) and liquid particles (blue) are calculated using virtual particle (green) concepts.

interaction forces ($\mathbf{F}^{ss}$) between solid particles, the modified Lennard-Jones (LJ) type forces are employed as

$$\mathbf{F}^{ss} = \frac{f_0^{ss}}{r^{ss}}\left[\left(\frac{r_0^{ss}}{r^{ss}}\right)^{13} - \left(\frac{r_0^{ss}}{r^{ss}}\right)^{7}\right], \tag{10}$$

where r^{ss} and r_0^{ss} are the present and the original distances between two solid particles while f_0^{ss} is the strength of the LJ contact for solid-solid interaction. These $\mathbf{F}^{ss}$ forces aid to avoid overlapping of solid particles with each other. In order to reduce the computational cost, a cut-off distance for the LJ force $\mathbf{F}^{ss}$ is set to $1.1r_0^{ss}$. As can be seen in Fig. 2, $\mathbf{F}_{cb}^{ss}$ and $\mathbf{F}_{cd}^{ss}$ are the interaction forces between the solid particle, c, and the solid particles, b and d, respectively.

The weight of the Fe_3O_4 nanoparticles is also incorporated to the model. From experiments,[1] it has been measured that the total mass of Fe_3O_4 nanoparticles required to coat a water droplet of 15 μl is about 4.9×10^{-7} kg. Assuming that the shape of this liquid marble is spherical, the areal density of Fe_3O_4 nanoparticles on the liquid droplet is approximated to be 0.0173 kg/m^2. Finally, all the forces are added together and the following equations are used to calculate the velocities and the positions of the particles at any time (t):

$$\mathbf{V}_{n+1} = \mathbf{V}_n + (\mathbf{F}_{total} - c\mathbf{V}_n) \times (\Delta t/m), \tag{11}$$

$$\mathbf{X}_{n+1} = \mathbf{X}_n + \mathbf{V}_{n+1}\Delta t, \tag{12}$$

where $\mathbf{X}_n$ and $\mathbf{V}_n$ are the position and velocity at step n, $\mathbf{X}_{n+1}$ and $\mathbf{V}_{n+1}$ are the position and velocity at step $n+1$, while Δt, m, and c are the time step, mass of the particle, and damping coefficient, respectively.

III. RESULTS AND DISCUSSION

A. Validation

In this study, a water droplet coated with superhydrophobic Fe_3O_4 nanoparticles is considered. The radius (r) of the initial water droplet is assumed to be 1.55 mm. This r value gives a water droplet of approximately 15 μl. The initial distance between two consecutive liquid particles l_i should be smaller enough to represent the realistic shape of the liquid marble. However, l_i cannot be too small since it affects the computational cost. Preliminary simulations showed that the liquid marble model with $l_i = 0.1 \times 10^{-3}$ m provides reasonably

stable and accurate results. Moreover, in this axis symmetrical model, the height, δz, and width, δy, of the liquid particles are also set to 0.1×10^{-3} m. However, if the l_i value is further reduced, Δt has to be also reduced. The other simulation parameters are set as in Table I.

It is assumed that the liquid marble is placed on the top of a horizontal flat substrate, and the frictional coefficient of the interface is assumed to be 0.1 [see Fig. 3(a)]. The following boundary condition is applied to the model in order to keep the liquid marble on the top of the solid substrate:

$$y^p = \begin{cases} y^p, & \text{if } y^p > y^{sub} \\ y^{sub}, & \text{if } y^p \le y^{sub}, \end{cases} \tag{13}$$

$$vy^p = \begin{cases} vy^p, & \text{if } y^p > y^{sub} \\ 0, & \text{if } y^p \le y^{sub} \text{ and } vy^p \le 0, \end{cases} \tag{14}$$

where y^p, vy^p, and y^{sub} are the y-component of the position vector of the particle of interest, y-component of the velocity vector of the particle of interest, and the y-coordinate of the solid substrate, respectively.

In this simulation, Δt and $\Delta t/m$ are set to 5×10^{-5} s and 5 s/kg, respectively. The damping coefficients, C, for solid (C_s) and liquid particles (C_l) are set to 1×10^{-2} N s/m and 5×10^{-2} N s/m, respectively. The LJ contact strength values, f_0^{sl} and f_0^{ss}, are set to 5×10^{-9} N/m and 2×10^{-9} N/m, respectively. It should be noted that both f_0^{sl} and f_0^{ss} are problem dependent parameters and have to be carefully chosen for a given problem. Since in this study r_0^{ss} is greater than r_0^{sl}, the f_0^{ss} value is set smaller compared to the f_0^{sl} value.

When the liquid marble deforms its shape from the circular shape, the perimeter of the circular liquid marble increases. As a result, the distances between consecutive solid particles increase. Therefore, in order to maintain uniform distances between consecutive solid particles, r_0^{ss} is updated by

$$r_0^{ss} = \frac{1}{n} \sum_{i=1}^{n} r^{ss}. \tag{15}$$

Simulation results show that the width (W) of the liquid marble increases while its height (h) decreases with time [see Fig. 3(b)]. As can be seen in Fig. 3(b) after about 1.5×10^8 iterations, the simulations reach a steady state and the shape [see Fig. 3(b)] of the liquid marble does not change with time anymore. The shape obtained from the simulation is highly comparable with the experimental data published by Zhao *et al.*[1] In order to validate the model, the morphology of the liquid marbles with different initial radii is studied. The radius, r, is set to 0.55, 1.05, 1.55, 2.05, 2.55, 3.05, 3.55, and 4.05 mm. All the other parameters are kept unchanged.

Simulation results show that smaller liquid marbles exhibit quasi-spherical shapes, while the larger liquid marbles exhibit puddle-like shapes [see Fig. 3(c)]. The comparison of model prediction and experimental results[1] confirms the extremely high accuracy of the model predictions.

B. Effect of the density of the liquid on the shape of the liquid marble

The densities of the most common liquids vary between 700 and 1300 kg/m^3. Therefore, the effect of the density of the liquid on the morphology of the liquid marble is studied. The density of the liquid is changed to 700, 800, 900, 1000, 1100, 1200, and 1300 kg/m^3. All the other parameters are kept unchanged. In order to compare the morphology of the liquid marbles with different densities, we define the Deformation Index (DI) as

$$DI = h/W. \tag{16}$$

As can be seen in Fig. 4(a), the simulation results show that the DI linearly increases with the density of the liquid. When the density of the liquid decreases, the effect of the surface tension becomes dominant and the liquid marble shows more spherical shape. On the other hand, when the density increases, the gravitational forces become dominant and the liquid marbles show more puddle-like shapes. When a liquid marble exhibits puddle-like shapes, the surface area to volume ratio of the liquid marble increases compared to that value of a spherical liquid marble with the same volume. Therefore, the amount of solid particles required to coat the liquid droplet increases. This model has the potential to be improved to predict the amounts of solid particles required to coat the liquid droplet with different densities. In addition to that, it is possible to predict the geometry of the liquid marbles with different densities and use the model predictions in designing microfluidic systems.

C. Effect of the surface tension of the liquid on the shape of the liquid marble

The surface tension of the most common liquids varies between 0.01 and 0.1 N/m. Therefore, the effect of the surface tension of the liquid on the morphology of the liquid marble is

TABLE I. Key simulation parameters for the model.

Parameter	Definition	Value
γ	Surface tension	0.072 N/m
ρ	Density	1000 kg/m^3
g	Acceleration of gravity	9.8 m/s^2
l_i	Initial distance between two consecutive liquid particles	0.1×10^{-3} m
δz	Height of liquid particles	0.1×10^{-3} m
δy	Width of liquid particles	0.1×10^{-3} m
d	Diameter of solid particles[1]	10.2×10^{-9} m
$r_0{}^{sl}$	Original distance between solid and liquid particles, $r_0{}^{sl} = (l_i + d)/2$	$0.050\,005\,1 \times 10^{-3}$ m
k_a	Area constraint coefficient	1×10^{-5} N m
k_l	Uniform length coefficient	1×10^{-5} N m

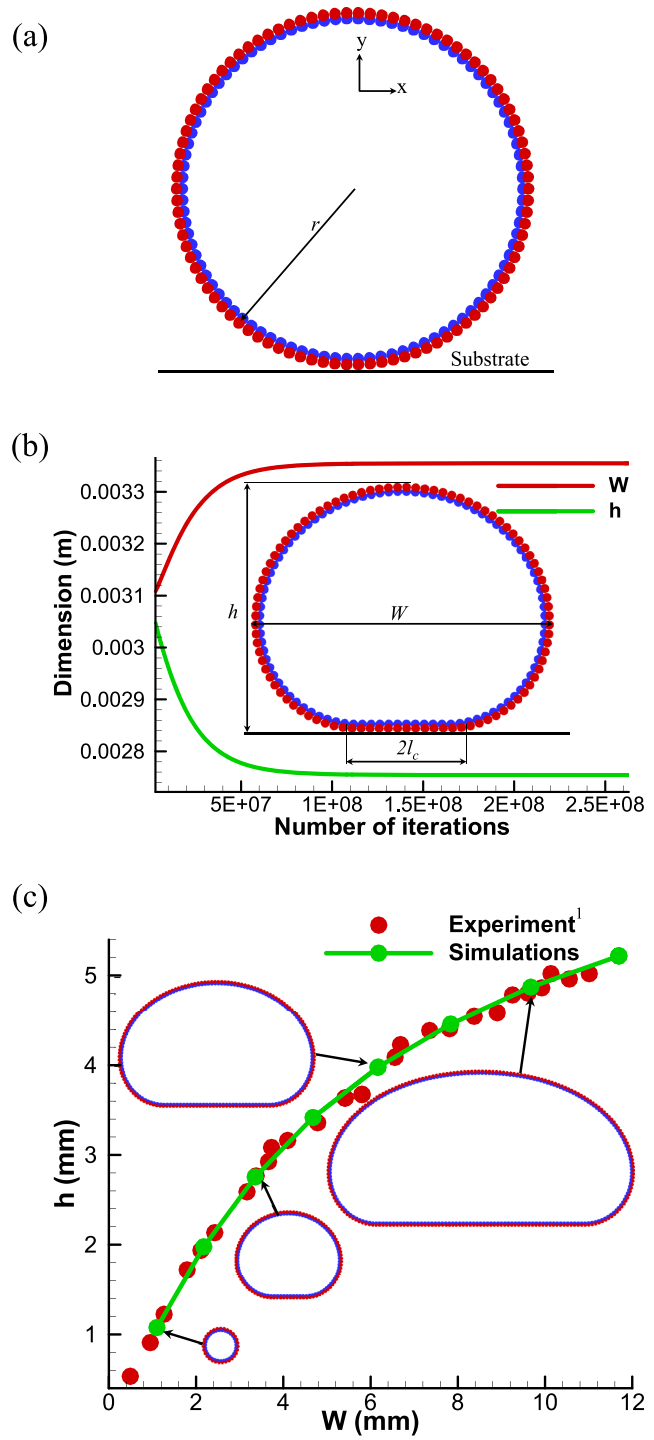

FIG. 3. (a) Initial particle configuration of the liquid marble (red and blue represent solid and liquid particles, respectively), (b) variation of width, W, and height, h, of the liquid marble of 15 μl with the number of iteration and final steady state shape of the liquid marble (here, l_c is the radius of the liquid marble's circular contact area), and (c) variation of height, h, of the liquid marbles of different sizes with their width, W.

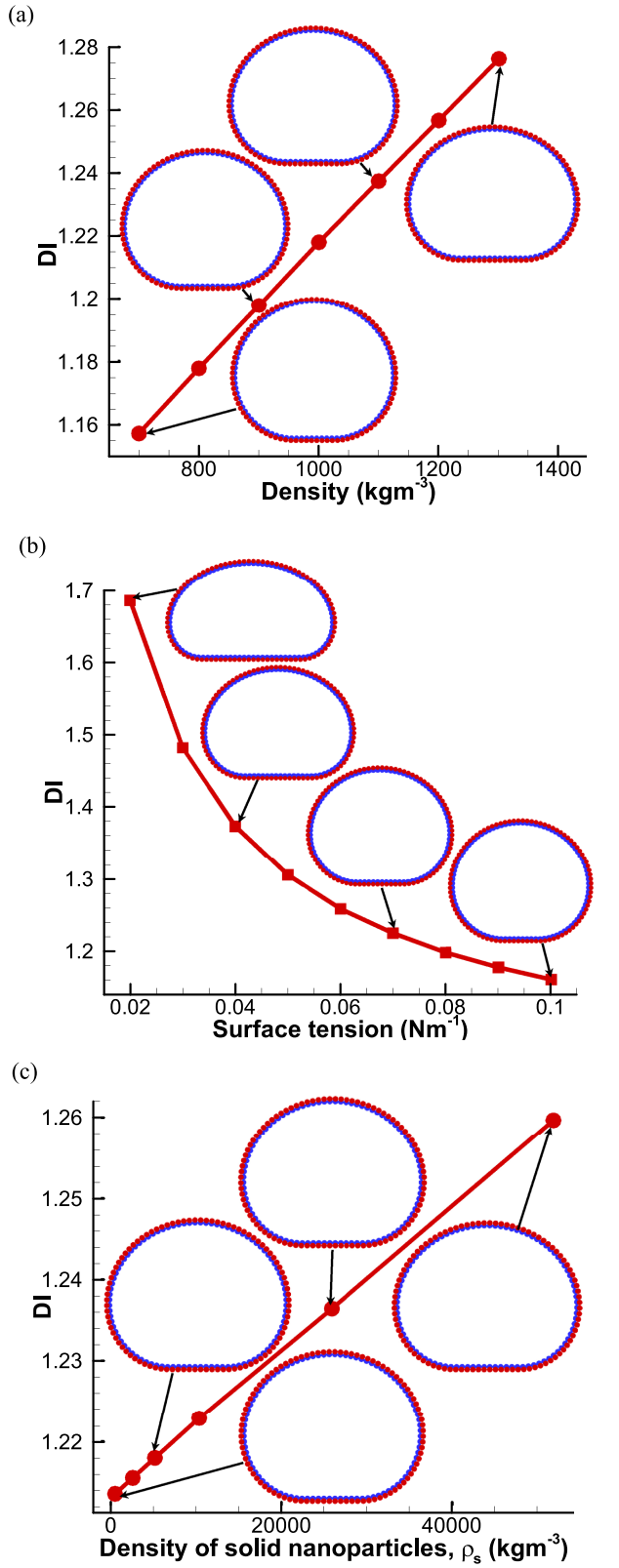

FIG. 4. The variation of DI of a 15 μl liquid marble against (a) the density of the liquid, (b) the surface tension of the liquid, and (c) the density of the coating material.

studied. The surface tension of the liquid is changed to 0.02, 0.03, 0.04, 0.05, 0.06, 0.07, 0.08, 0.09, and 0.1 N/m. All the other parameters are kept unchanged. When the surface tension of the liquid is low, the forces acting on the liquid to prevent the dispersion of liquid become smaller compared to the gravitational forces and the liquid marble shows puddle shapes [see Fig. 4(b)]. The model predicts that the DI of the liquid marble exponentially decreases with the surface tension of the liquid [see Fig. 4(b)]. It can be predicted that for extremely high surface tension values, the DI of the liquid marble should reach 1.0, i.e., spherical.

The geometrical shapes obtained from the developed model could be easily used to predict the behavior of the liquid marbles in fluid flows. Thereby, the potential of the liquid marbles for the drug delivery process in the human cardiovascular network could be evaluated.

D. Effect of weight of the coating material on the shape of the liquid marble

The effect of the weight of the nanoparticles on the morphology of the liquid marbles is studied. In previous simulations, Fe_3O_4 nanoparticles were used to coat the liquid droplet and the density (ρ_{s0}) of the coating material was set to 5.18×10^3 kg/m^3. In this simulation, the density of the nanoparticles (ρ_s) is changed to $0.1\rho_{s0}$, $0.5\rho_{s0}$, ρ_{s0}, $2\rho_{s0}$, $5\rho_{s0}$, and $10\rho_{s0}$ to represent different nanoparticles with different density values. All the other parameters are kept unchanged. As can be seen in Fig. 4(c), the *DI* of the liquid marbles linearly increases with the density of the nanoparticles (ρ_s). This variation is very similar to the change in *DI* with the density of the liquid. However, it can be seen from Figs. 4(a) and 4(c) that the two graphs have different slopes. The slope of the graph in Fig. 4(a) (1.98×10^{-4} m^3/kg) is higher than that value of the graph in Fig. 4(c) (8.99×10^{-7} m^3/kg). Therefore, it can be concluded that the effect of the density or the weight of the nanoparticles is negligible in determining the shape of the liquid marble compared to the effect of the density of the liquid. Therefore, the coating materials for liquid droplets can be chosen according to the application of the liquid marbles irrespective of the coating material's density. However, this model could be easily used to accurately predict the geometrical shapes of the liquid marbles with different types of coatings with extreme densities.

E. Non-dimensional scaling analysis

It was shown in Sec. III D that the effect of the weight of the coating material on the morphology of the liquid marble can be neglected. Therefore the dominance of the gravitational energy over the surface energy of the liquid marbles is represented by the Bond number,

$$\mathrm{Bo} = \frac{\rho g r^2}{\gamma}. \tag{17}$$

It should be noted that r is the radius of the un-deformed liquid marble, which can be calculated by $r = (3V/4\pi)^{1/3}$, where V is the volume of the liquid marble. In this model, r is exactly equal to the radius of the initial circle. As can be seen in Eq. (17), Bo varies with the changes in γ, ρ, and r. Therefore, the variations of the liquid marble shape are directly related to Bo. When Bo increases, the gravitational energy of the liquid marble increases, and as a result, the height of the liquid marble decreases. With the aid of combined analytical and experimental approaches, a relationship between the dimensionless height, $h^* = h/r$, and Bo of the liquid marble has been derived[22,23] as

$$h^* = \begin{cases} 2 & \text{for smaller liquid marbles(Bo} << 1) \\ 2\mathrm{Bo}^{-1/2} & \text{for larger liquid marbles(Bo} \geq 1) \end{cases}. \tag{18}$$

Using the simulation results in Secs. III A–III C, the $h*$ value is calculated and plotted against Bo, in Fig. 5(a). Figure 5(a) shows that our numerical model follows the above scaling laws.

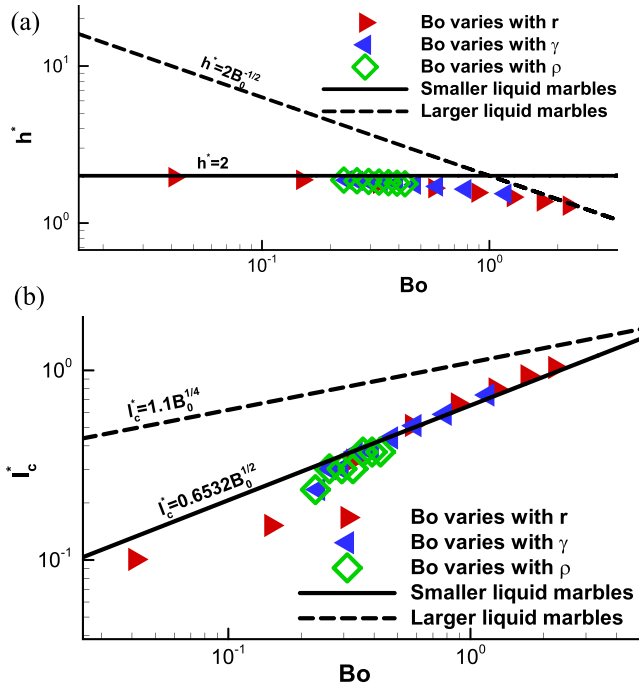

FIG. 5. The variation of (a) the dimensionless height, h^*, and (b) the dimensionless radius of the circular contact area, $l_c{}^*$, of the liquid marbles against the Bond number, Bo.

On the other hand, when Bo increases, the width and the contact area of the liquid marble increase. Mahadevan and Pomeau[24] derived a scaling law to express the relationship between the radius of the circular contact area of a liquid droplet and Bo,

$$l_c \sim \mathrm{Bo}^{1/2} r, \tag{19}$$

where l_c is the radius of the circular contact area of the liquid marble [see Fig. 3(b)] and $\sim$ stands for "of the order of."[24] The dimensionless form of the above relationship can be formulated for a liquid marble as[22]

$$l_c{}^* = l_c/r \sim \mathrm{Bo}^{1/2}, \tag{20}$$

where l_c* is the dimensionless radius of the liquid droplet's circular contact area. Aussillous and Quéré[23] reported that when Bo ≥ 1 the liquid marbles take puddle-like shapes and the radius of the liquid marble's circular contact area scales with $\mathrm{Bo}^{1/4}$,

$$l_c{}^* \sim \mathrm{Bo}^{1/4}. \tag{21}$$

Again, the simulation results in Secs. III A–III C are used to calculate $l_c{}^*$ and plotted against Bo in Fig. 5(b). Nguyen[22] experimentally found that $l_c{}^* = 1.1\mathrm{Bo}^{1/4}$ for the liquid marbles with larger Bo. However, in this study, most of the liquid marbles have smaller Bo (Bo ≤ 1). Therefore, we employ the scaling law derived for smaller liquid marbles. Using Matlab curve fitting tools, it was found that the model predictions can be fitted to $l_c{}^* = 0.653\mathrm{Bo}^{1/2}$ with a root mean square error (RMSE) of 0.0521. Therefore, it can be concluded that the model predictions follow the scaling laws.

TABLE II. Density and surface tension values of different liquids.

Liquid	Density (kg/m^3)	Surface tension (N/m)
Water	1000	0.0720
DMSO	1100	0.0435
Toluene	867	0.0284
Ethanol	789	0.0221
Octane	703	0.0216

F. Shape of the liquid marbles of different liquids

In this section, we present the results obtained from liquid marbles with different liquids. Earlier, we demonstrated the effects of density and the surface tension of the liquid on their shapes independently. In this section, both the density and surface tension of the liquid are changed by employing five types of liquids: water, dimethyl sulfoxide (DMSO), toluene, ethanol, and octane. The density and the surface tension of the above liquids are as follows in Table II. The density and the surface tension of the model are changed according to the properties of the above liquids. The initial radius of the circle is set to 1.55 mm, which gives the liquid droplet a volume of approximately 15 μl. All the other parameters are kept unchanged.

Simulation results show that the shapes of the liquid marble change with both the density and the surface tension. Among all five liquid marbles, the liquid marble of water shows more spherical shape compared to the other liquid marbles (see Fig. 6). It can be seen that the proposed model is capable of predicting the shape of the liquid marbles with different liquids and different coatings. This model will reduce the experimental cost and will inspire new experiments.

G. Opening and closing of magnetic liquid marbles under magnetic force

In this simulation, a water droplet of 15 μl coated with super-hydrophobic Fe_3O_4 nanoparticles is considered. First, the steady state shape of the liquid marble at rest is obtained. At this stage, the distance between consecutive solid particles is the natural distance between them, and as long as there is no external force acting on them, it remains constant. Therefore r_0^{ss} is not updated after obtaining the steady state shape at rest and is set to the distance between consecutive solid particles at rest. Here, the areal volume of Fe_3O_4 nanoparticles on the water droplet is approximated from the experiments[1] to be 3.35×10^{-6} m. The total magnetic force acting on a magnetic liquid marble can be calculated by

$$F_{\text{mag}} = \frac{V\Delta\chi}{\mu_0}(\nabla B)\,B, \tag{22}$$

where V is the total volume of Fe_3O_4 nanoparticles, $\Delta\chi$, μ_0, B, and ∇B are the difference in magnetic susceptibilities between the nanoparticle and the surrounding medium, the permeability of vacuum, magnetic flux density, and magnetic field gradient, respectively.

In this study, $\Delta\chi$ and μ_0 are assumed to be 1.45 and $4\pi \times 10^{-7}$ T m/A as in the experiments.[1] The experimentally measured[1] variation of B with the distance from magnet surface [see Fig. 7(a)] is used in this simulation. In order to determine B and ∇B values from Fig. 7(a), the distance from magnet surface ($\bar{y}$) is calculated by

$$\bar{y} = \frac{1}{n}\sum_{i=1}^{n} y_s, \tag{23}$$

where y_s is the distance from the magnet surface to each solid particle [see Fig. 7(b)].

Finally, the total force calculated by Eq. (22) is equally divided among all the solid particles. The magnet is placed under the flat solid substrate with a gap (y_m) of 1 mm. Preliminary simulation results provided slightly deformed liquid marbles with no opening from the top of the liquid marble. This was due to the higher LJ contact strength values, f_0^{sl} and f_0^{ss}, which are problem dependent parameters. In order to get simulation results comparable with the experimental findings,[1] f_0^{sl} and f_0^{ss} are adjusted to 5×10^{-10} N/m and 3×10^{-10} N/m, respectively. The adjusted f_0^{sl} and f_0^{ss} provide LJ forces with the magnitude of the same scale with the magnetic forces.

1. Dimensional analysis

Simulation results reveal that the solid particles are pulled down toward the substrate by the magnetic forces acting on them. Due to that, the height of the liquid marble decreases, while its width increases gradually [see Fig. 7(c)]. After about 2.2×10^7 iterations, the liquid marble begins to open to the atmosphere from the top, and after about 2.0×10^8, it reaches a steady state with a significant opening [see Fig. 8(b)]. As long as the magnetic forces are applied on the solid particles, it remains opened. It can be seen from Fig. 8(b) that the reduction in height and increment in width of the liquid marble are rather noticeable due to the application of the magnetic force. Further, the contact area of the liquid marble with the substrate has been increased [see Fig. 8(b)]. However, once the magnet is removed, solid particles move back to almost their original positions and close the opening. However, a closer look at Fig. 8(c) shows that there is still a tiny opening of the liquid marble, which is negligible in comparison to the distance between particles modeling the coating nanoparticles. This is a numerical error which occurs due to the representation of a cluster of Fe_3O_4 nanoparticles by one numerical solid particle in the model. This error could be minimized by further discretizing the solid particles so that it increases the number of solid particles in the problem domain. However, it should be noted that the computational cost increases with the

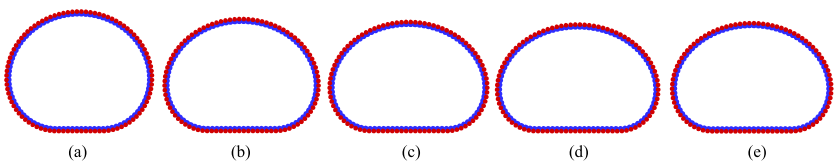

FIG. 6. Shape of liquid marbles of 15 μl of (a) water, (b) DMSO, (c) toluene, (d) ethanol, and (e) octane.

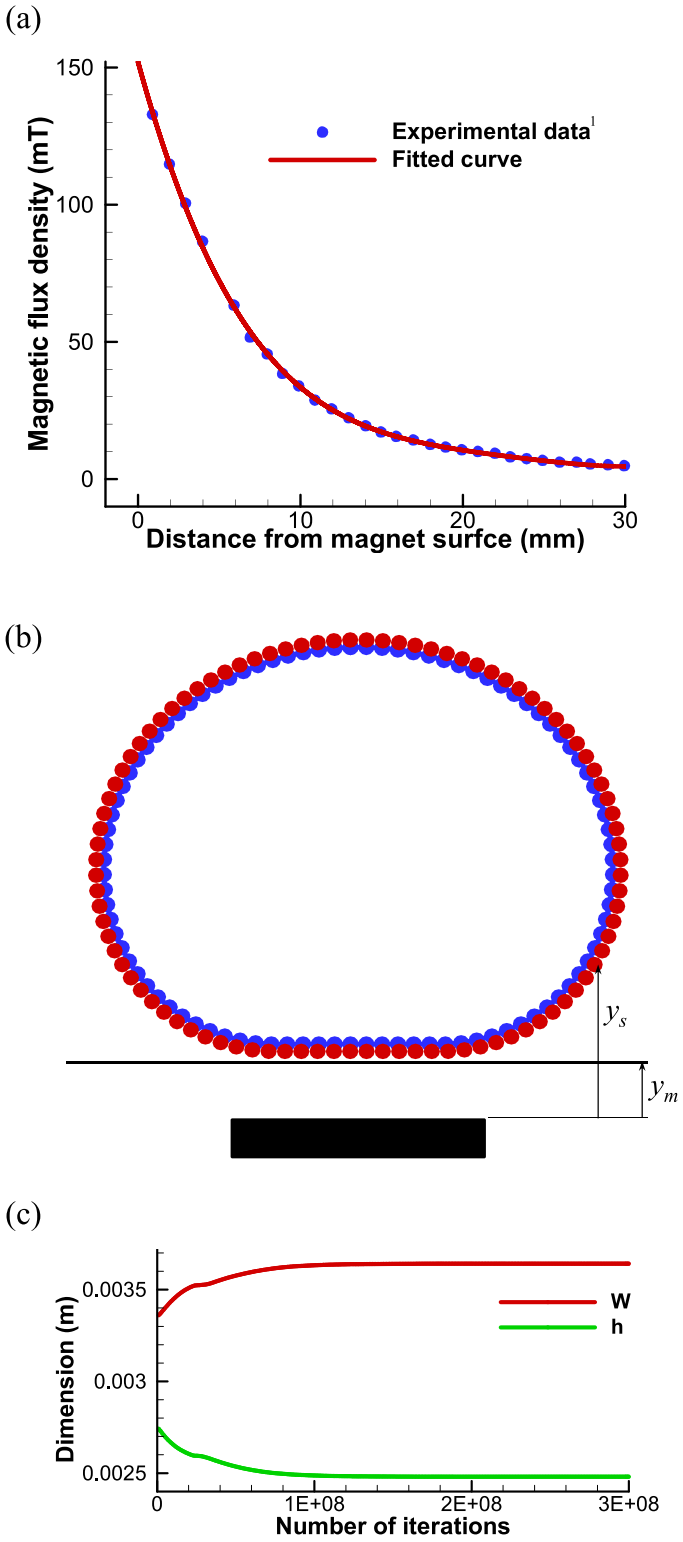

FIG. 7. (a) The variation of magnetic flux density against the distance measured from magnetic surface. (b) The magnet is placed under the substrate with a gap of y_m, and (c) the variation of the width, W, and the height, h, of the magnetic liquid marble of 15 μl with the number of iteration, when a magnet is present.

number of particles and that the general accuracy of this preliminary model was found adequate at this stage to not require further increase in particle number. In addition to that, once the magnet is removed, the height of the liquid marble increases and reaches its initial height at rest. On the other hand, the width of the liquid marble decreases back to its original value. The simulation results are highly comparable with the experimental results.[1] This feature of the liquid marble could be used in drug delivery, and this model has a high potential in investigating the optimum opening to release the liquid from the liquid marble in the drug delivery process.

Finally, the behavior of the magnetic liquid marbles of 15 μl is studied by changing the distance between the substrate and the magnet (y_m). Here, y_m is changed to 0, 0.5, 1.0, 1.5, and 2.0 mm. All the other parameters are unchanged.

Simulation results show that the *DI* of the liquid marble increases when the magnet is placed closer to the substrate [see Fig. 9(a)]. Similar behavior is observed in the width of

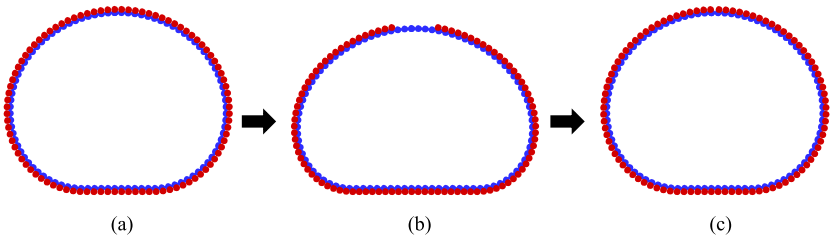

FIG. 8. The steady state shape of the magnetic liquid marble of 15 μl (a) at rest, (b) when the magnet is present, and (c) when the magnet is removed; blue represents liquid particles, and red represents solid particles.

the opening as well. As can be seen in Fig. 9(b), the width of the opening increases when the magnet is closer to the substrate.

However, it can be concluded that the width of the opening could be further increased by introducing a magnet with a higher magnetic flux density. It is evident that this model can be used to measure the width of the opening of magnetic liquid marbles under different magnets. Without carrying out intensive experiments, which are always associated with extremely higher costs, this model could be easily used to predict the opening behavior and measure the width of the opening of the liquid marbles under different environmental conditions.

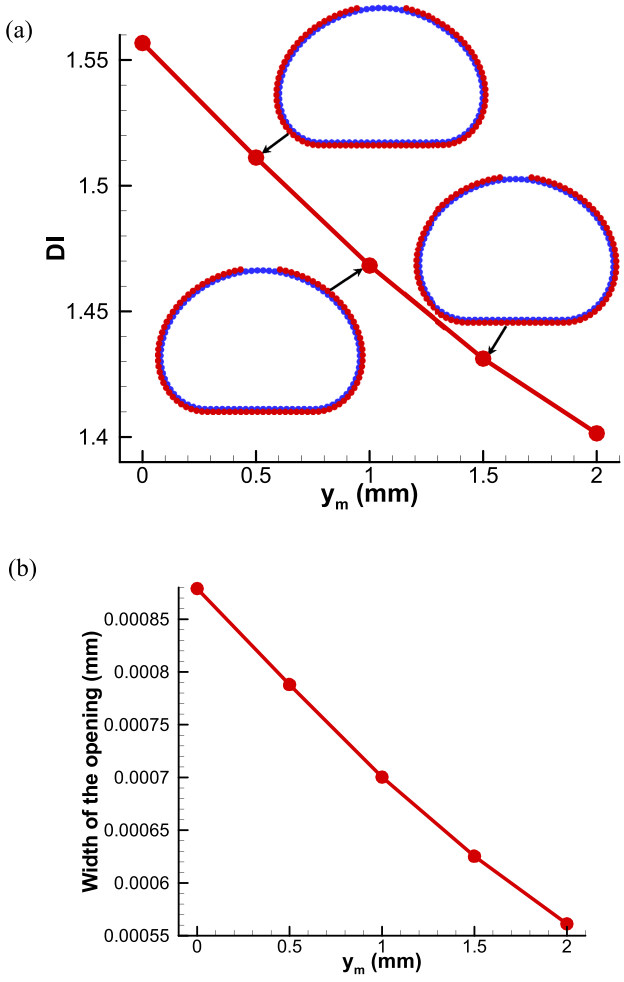

FIG. 9. The variation of (a) the *DI* and (b) the width of the opening of the liquid marble of 15 μl with the distance between the substrate and the magnet (y_m).

2. Non-dimensional analysis

The magnetic Bond number (Bm) can be employed to perform a non-dimensional analysis for geometrical parameters of liquid marbles. The magnetic Bond number of ferrofluid marbles is defined by the relative ratio between magnetic energy and surface energy,

$$\mathrm{Bm} = \frac{rMB}{\gamma}, \tag{24}$$

where M is the magnetization density of the ferrofluid. However, this equation [Eq. (24)] is only applicable for the ferrofluid marbles. Since this study is carried out with the water droplets coated with Fe_3O_4 nanoparticles, quasi-surface forces of magnetic coating have to be taken into account, and Eq. (24) is not appropriate to calculate Bm. Therefore, an alternative way is required to define Bm, and we introduce the apparent magnetic surface tension (γ_a). γ_a is the equivalent surface tension of the deformed (due to the magnetic forces) liquid marble, which gives the same deformed shape even without any magnetic force. γ_a is calculated by matching the *DI*s of a magnetic liquid marble when it is affected by a magnetic field and when it is not. With the aid of model predictions in Sec. III C, a curve is fit (see Fig. 10) to describe the relationship between the *DI* and the surface tension of a liquid marble of 15 μl with no magnetic force. Then, γ_a values of deformed (due to the magnetic forces) liquid marbles are calculated using their *DI*s [*DI*s are extracted from Fig. 9(a)]. The calculated γ_a

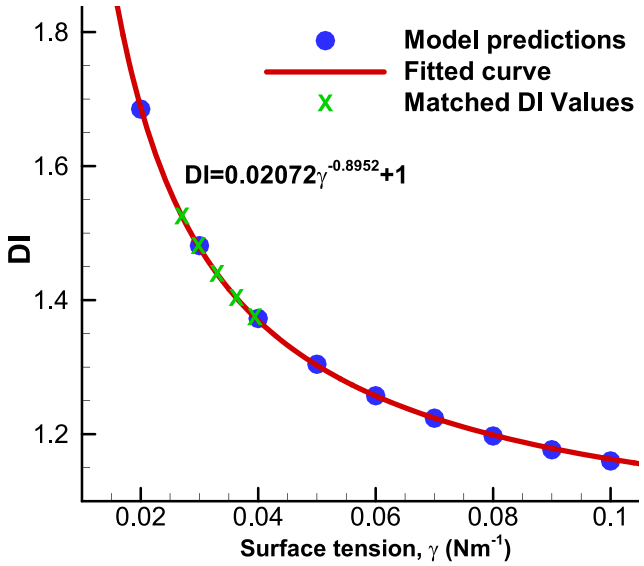

FIG. 10. Fitted curve for the variation of the *DI* against the surface tension of the liquid marble. Here X represents the points related to the *DI*s of the deformed magnetic liquid marbles.

is used to calculate Bm by

$$\mathrm{Bm} = \frac{\rho g r^2}{\gamma_a}. \tag{25}$$

Finally, h^* and l^* are calculated and plotted against Bm (see Fig. 11). As can be seen in Fig. 11, the model predictions comply with the scaling laws.

H. Compressibility of the liquid marbles

The liquid marbles are soft elastic solid objects,[1] which can be compressed under external loadings. In this section, the compressibility of a water droplet of 15 μl coated with super-hydrophobic Fe_3O_4 nanoparticles is assessed. As can be seen in Fig. 12(a), a horizontal plate is used to compress the liquid marble. The horizontal plate is vertically moved down by 0.02 mm after every 1×10^7 iterations. The following boundary conditions are applied to model the compressing process of the liquid marble:

$$y^p = \begin{cases} y^p, & \text{if } y^p < y^{plate} \\ y^{plate}, & \text{if } y^p \geq y^{plate}, \end{cases} \tag{26}$$

$$vy^p = \begin{cases} vy^p, \text{ if } y^p < y^{plate} \\ 0, \quad \text{if } y^p \geq y^{plate} \text{ and } vy^p \geq 0, \end{cases} \tag{27}$$

where y^{plate} is the y-coordinate of the virtual horizontal plate. The movement of the virtual horizontal plate is stopped when it reaches the required compression. In the steady state, the sum of the y-component of the forces, f^v, acting on the particles is calculated. The stress, σ, and strain, ε, of the liquid marble are then calculated by

$$\sigma = \frac{f^v}{W_c \delta z}, \tag{28}$$

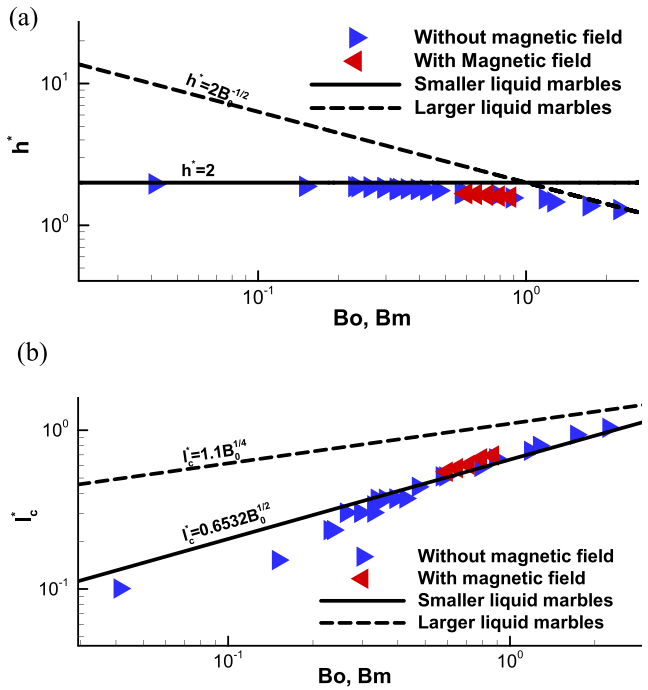

FIG. 11. Variation of (a) the dimensionless height, h^*, and (b) the dimensionless radius of the circular contact area, l_c^*, of the liquid marble against the Bond numbers, Bo and Bm.

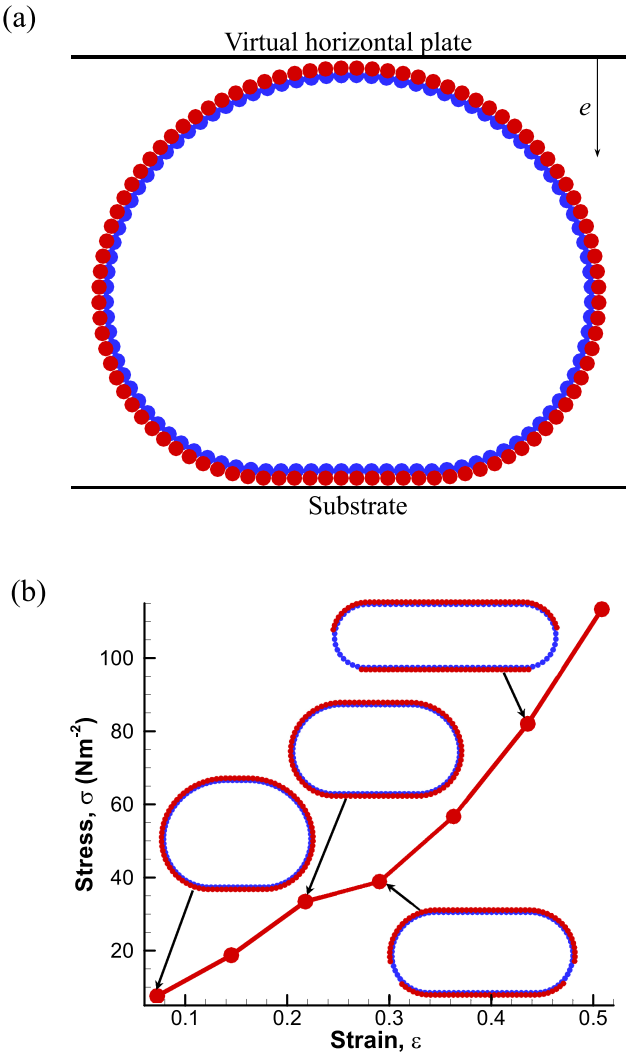

FIG. 12. (a) A virtual horizontal plate is moved vertically downwards to compress a magnetic liquid marble of 15 μl and (b) the stress strain curve of the liquid marble.

$$\varepsilon = \frac{e}{h_0}. \tag{29}$$

It should be noted that W_c in Eq. (28) and h_0 in Eq. (29) are the width of the compressed magnetic liquid marble and the height of the uncompressed liquid marble, respectively, while e is the displacement of the virtual horizontal plate.

Figure 12(b) shows that the variation of the stress against the strain of the liquid marble. At low compressions, the stress linearly increases with the strain. However, if the strain exceeds approximately 0.25, cracks start to appear on the liquid marble and a sudden reduction in the stress can be observed [Fig. 12(b)]. At higher compressions, stress again increases with the strain, but it occurs at a higher rate compared to the low compressions. At low compressions ($\varepsilon < 0.2$), the elastic modulus of the liquid marble is calculated to be 177.39 Pa. However, the proposed model is not able to simulate the compression of the liquid marbles when $\varepsilon > 0.5$. This model has the potential to be improved to predict the toughness and shear modulus of different liquid marbles, which could be used in designing microfluidic systems.

IV. CONCLUSIONS

A novel numerical model was developed to predict the behavior of magnetic liquid marbles. This model is computationally highly efficient since it models only the surface layer of the liquid and the solid nanoparticles. The surface tension and the gravitational forces were taken into account. The model predictions are highly comparable with experimental results. This particle model is capable of simulating opening and closing of magnetic liquid marbles under the presence of a magnet. The developed model predicts that the width of the opening of the magnetic liquid marble can be controlled by the properties of the magnet. Moreover, the scaling analysis shows that the model predictions are consistent with the scaling laws. The proposed model predicts the elastic modulus of a water droplet coated with Fe_3O_4 nanoparticle liquid marble to be 177.39 Pa at low compressions. The proposed modeling approach has the potential to be a powerful tool to predict the behavior of magnetic liquid marbles serving as bioreactors.

ACKNOWLEDGMENTS

Support provided by the High Performance Computer (HPC) resources in Queensland University of Technology (QUT) is gratefully acknowledged. The Australian Research Council (ARC) is acknowledged for its financial support with Grant Nos. ARC-DECRA DE130101183, LP150100737, DP150100828, and DP170100277.

APPENDIX: SELECTION OF KEY SIMULATION PARAMETERS

1. l_i (initial distance between two consecutive liquid particles), δz (height of liquid particles), and δy (width of liquid particles) = 0.1×10^{-3} m

These are the geometrical parameters of the liquid particles. Here, the values should be small enough to obtain accurate results (similar in finite element modeling; finer the mesh, the more accurate the results). However, l_i, δz, and δy cannot be set too small since it is computationally expensive. Preliminary simulations with $l_i = \delta z = \delta y = 0.1 \times 10^{-3}$ m provided accurate results with a reasonable computational efficiency in the process of validation. Therefore, the authors decided to keep these values.

2. d (diameter of solid particles) = 0.1×10^{-3} m

Experimentally[1] it was found that the Fe_3O_4 particles are roughly spherical and they have an average size of 10.2 ± 2.7 nm. Therefore, in this work, we set d to 10.2×10^{-9} m.

3. r_0^{sl} (*original distance between solid and liquid particles*) = $(l_i + d)/2 = 0.050\,005\,1 \times 10^{-3}$ m

r_0^{sl} is the addition of half of l_i (initial distance between two consecutive liquid particles) and half of d (diameter of solid particles). As explained earlier, l_i is a set value and d is an experimentally[1] extracted value. This means that the solid and liquid numerical particles are in contact.

4. K_a (area constraint coefficient) = 1×10^{-5} N m

In order to conserve the volume of the liquid droplet, the area enclosed by the particles is conserved and the formula used in red blood cell modeling[20] is used to calculate the forces acting on each particle due to the areal conservation by Eq. (1). The purpose of using this equation is to maintain a constant area throughout the whole simulation. As can be seen in Eq. (1), $\mathbf{F}^a$ is zero when there is no area change (i.e., $A = A_0$). Therefore, at the steady state, if the difference between A and A_0 is insignificant (i.e., the area is conserved), there is no effect from $\mathbf{F}^a$. However, the k_a value should be chosen such that Eq. (1) does not generate large $\mathbf{F}^a$ forces, which make the model unstable (if k_a is too high, in order to make the model stable, the time step, Δt, has to be reduced, and it is computationally inefficient). Moreover, if the k_a value is too small, Eq. (1) will not produce large enough $\mathbf{F}^a$ forces to conserve the area of the liquid droplet. Preliminary simulations with $k_a = 1 \times 10^{-5}$ N m provided reasonably accurate results. Therefore, in this work, k_a is set to 1×10^{-5} N m for remaining simulations.

5. K_l (uniform length coefficient) = 1×10^{-5} N m

Due to the area conservation, the distances between consecutive liquid particles increase, when the liquid droplet shows any shape other than a circle. Therefore, in order to maintain a uniform distance between consecutive liquid particles, interaction forces ($\mathbf{F}^{ff}$) are introduced by Eq. (2). The purpose of using this concept is to maintain a uniform distance between consecutive liquid particles. Since these forces are acting in the opposite direction but equal in magnitude on neighboring particles, there is no resultant force acting on the liquid marble at any stage of the simulation. Moreover, at the steady state, l is equal to l_0 and there is no effect from Eq. (2). In this case also, an optimum value (similar to choosing k_a) should be chosen for k_l such that it provides accurate results with acceptable computational efficiency. Preliminary simulations with $k_l = 1 \times 10^{-5}$ N m provided reasonably accurate results. Therefore, in this work, k_l is also set to 1×10^{-5} N m for remaining simulations.

6. f_0^{sl} (the strength of the LJ contact for solid-liquid interaction) = 5×10^{-9} N/m

The Lennard Jones (LJ) forces are commonly used[25–27] to represent the interaction between particles. Therefore, in this work, the interaction between solid and liquid particles is represented by LJ forces [see Eq. (9)]. These LJ forces are acting pair-wisely in the opposite directions on solid and liquid particles. The application of LJ type forces is more appropriate in order to avoid the penetration of solid particles through the liquid surface. Furthermore, these forces aid to maintain a constant gap between solid and liquid particles.

An optimum value (similar to choosing k_a, and k_l) should be chosen for f_0^{sl} such that it provides accurate and steady results with no penetration of solid particles through the liquid surface. Preliminary simulations with $f_0^{sl} = 5 \times 10^{-9}$ N m^{-1} provided accurate results with high computational efficiency. Therefore, in this work, f_0^{sl} is also set to 5×10^{-9} N/m for remaining simulations.

7. f_0^{ss} (the strength of the LJ contact for solid-solid interaction) = 2×10^{-9} N/m

The Lennard Jones (LJ) forces are also used to model the interaction between solid particles [see Eq. (10)]. The $\mathbf{F}^{ss}$ forces in Eq. (10) aid to avoid overlapping of solid particles with each other. Preliminary simulations with $f_0^{ss} = 2 \times 10^{-9}$ N/m provided accurate results with high computational efficiency. Therefore, in this work, f_0^{ss} is also set to 2×10^{-9} N m^{-1} for remaining simulations.

[1] Y. Zhao, Z. Xu, M. Parhizkar, J. Fang, X. Wang, and T. Lin, "Magnetic liquid marbles, their manipulation and application in optical probing," Microfluid. Nanofluid. **13**(4), 555–564 (2012).

[2] C. H. Ooi, R. K. Vadivelu, J. St John, D. V. Dao, and N.-T. Nguyen, "Deformation of a floating liquid marble," Soft Matter **11**(23), 4576–4583 (2015).

[3] P. Aussillous and D. Quéré, "Liquid marbles," Nature **411**(6840), 924–927 (2001).

[4] M. Newton, D. Herbertson, S. Elliott, N. Shirtcliffe, and G. McHale, "Electrowetting of liquid marbles," J. Phys. D: Appl. Phys. **40**(1), 20 (2006).

[5] G. McHale and M. Newton, "Liquid marbles: Topical context within soft matter and recent progress," Soft Matter **11**(13), 2530–2546 (2015).

[6] U. Cengiz and H. Y. Erbil, "The lifetime of floating liquid marbles: The influence of particle size and effective surface tension," Soft Matter **9**(37), 8980–8991 (2013).

[7] Y. Xue, H. Wang, Y. Zhao, L. Dai, L. Feng, X. Wang, and T. Lin, "Magnetic liquid marbles: A "precise" miniature reactor," Adv. Mater. **22**(43), 4814–4818 (2010).

[8] E. Bormashenko, "New insights into liquid marbles," Soft Matter **8**(43), 11018–11021 (2012).

[9] E. Bormashenko, R. Pogreb, and A. Musin, "Stable water and glycerol marbles immersed in organic liquids: From liquid marbles to Pickering-like emulsions," J. Colloid Interface Sci. **366**(1), 196–199 (2012).

[10] E. Bormashenko, "Liquid marbles: Properties and applications," Curr. Opin. Colloid Interface Sci. **16**(4), 266–271 (2011).

[11] E. Bormashenko and A. Musin, "Revealing of water surface pollution with liquid marbles," Appl. Surf. Sci. **255**(12), 6429–6431 (2009).

[12] S. Fujii, S. Kameyama, S. P. Armes, D. Dupin, M. Suzaki, and Y. Nakamura, "pH-responsive liquid marbles stabilized with poly (2-vinylpyridine) particles," Soft Matter **6**(3), 635–640 (2010).

[13] J. Tian, T. Arbatan, X. Li, and W. Shen, "Porous liquid marble shell offers possibilities for gas detection and gas reactions," Chem. Eng. J. **165**(1), 347–353 (2010).

[14] R. K. Vadivelu, C. H. Ooi, R.-Q. Yao, J. T. Velasquez, E. Pastrana, J. Diaz-Nido, F. Lim, J. A. Ekberg, N.-T. Nguyen, and J. A. St John, "Generation of three-dimensional multiple spheroid model of olfactory ensheathing cells using floating liquid marbles," Sci. Rep. **5**, 15083 (2015).

[15] M. K. Khaw, C. H. Ooi, F. Mohd-Yasin, R. Vadivelu, J. St John, and N.-T. Nguyen, "Digital microfluidics with a magnetically actuated floating liquid marble," Lab Chip **16**(12), 2211–2218 (2016).

[16] Y. Zhang and N.-T. Nguyen, "Magnetic digital microfluidics -a review," Lab Chip **17**(6), 994–1008 (2017).

[17] C. Y. H. Wong, M. Adda-Bedia, and D. Vella, "Non-wetting drops at liquid interfaces: From liquid marbles to Leidenfrost drops," Soft Matter **13**, 5250 (2017).

[18] H.-N. Polwaththe-Gallage, Y. Gu, S. C. Saha, W. Senadeera, and A. Oloyede, "Numerical simulation of red blood cells' motion: A review," edited by I. Gu, Y. Tong, and S. C. Saha, in 4th International Conference on Computational Methods (ICCM, 2012), available at https://eprints.qut.edu.au/56983/1/ICCM2012-236.pdf (2012).

[19] J. Monaghan and A. Kocharyan, "SPH simulation of multi-phase flow," Comput. Phys. Commun. **87**(1-2), 225–235 (1995).

[20] H.-N. Polwaththe-Gallage, S. C. Saha, E. Sauret, R. Flower, and Y. Gu, "A coupled SPH-DEM approach to model the interactions between multiple red blood cells in motion in capillaries," Int. J. Mech. Mater. Des. **12**(4), 477–494 (2016).

[21] H. C. P. Karunasena, W. Senadeera, R. J. Brown, and Y. T. Gu, "A particle based model to simulate microscale morphological changes of plant tissues during drying," Soft Matter **10**(29), 5249–5268 (2014).

[22] N.-T. Nguyen, "Deformation of ferrofluid marbles in the presence of a permanent magnet," Langmuir **29**(45), 13982–13989 (2013).

[23] P. Aussillous and D. Quéré, "Properties of liquid marbles," Proc. R. Soc. London, Ser. A **462**, 973 (2006), available at http://www.jstor.org/stable/pdf/20208922.pdf.

[24] L. Mahadevan and Y. Pomeau, "Rolling droplets," Phys. Fluids **11**(9), 2449–2453 (1999).

[25] J. J. Monaghan, "Simulating free surface flows with SPH," J. Comput. Phys. **110**(2), 399–406 (1994).

[26] F. Fleissner and P. Eberhard, "Load balanced parallel simulation of particle-fluid dem-sph systems with moving boundaries," in *Parallel Computing: Architectures, Algorithms and Applications* (IOS Press, 2008), Vol. 38, pp. 37–44, available at https://books.google.com.au/books?hl=en&lr=&id=WCOTC2UmXT8C&oi=fnd&pg=PA37&dq=Florian+Fleissner&ots=89h0FRftlq&sig=3DYeyDw8McGhNMxamdHraDrM92Y#v=onepage&q=Florian%20Fleissner&f=false.

[27] H. Schechter and R. Bridson, "Ghost SPH for animating water," ACM Trans. Graphics **31**(4), 61 (2012).